International Conference
Nuclear Energy for New Europe 2010
September 6-9, 2010, Portorož, Slovenia

Appropriate Thermodynamic Cycles to be Used in Future Pressure-Channel Supercritical Water-Cooled Nuclear Power Plants

Laure Lizon-A-Lugrin, Alberto Teyssedou
Nuclear Engineering Institute, Engineering Physics Department,
École Polytechnique de Montréal, Montréal, Québec
laure.lizon-a-lugrin@polymtl.ca, alberto.teyssedou@polymtl.ca

Igor Pioro
Faculty of Energy Systems and Nuclear Science,
University of Ontario Institute of Technology, Oshawa, Ontario
Igor.Pioro@uoit.ca

ABSTRACT

As member of the Generation IV International Forum (GIF), Canada has decided to orient its efforts towards the design of a CANDU-type SuperCritical Water-cooled nuclear Reactor (SCWR). Such a system must run at a coolant outlet temperature of about 625°*C* and at a pressure of 25 *MPa*. Even though several steam-cycle arrangements used in existing thermal-power plants have been discussed by many authors, none of the proposed cycles have been optimized and adapted to the pressure-channel SCWR concept. The present work is intended to fulfil this gap by including at least two alternative solutions of SCWR power cycles that could reheat the supercritical water in the reactor core to achieve a net mechanical power of 1200-*MW*. Thus, thermodynamic models for preselected power cycles, their validation among existing data as well as their optimization using an "evolutionary optimization" technique based on genetic algorithms are presented and discussed.

1 INTRODUCTION

The International Atomic Energy Agency (IAEA) has recently stipulated that by the year 2030 world primary-energy requirements will increase by up to 45%. To assure both a healthy world economy as well as adequate social standards, in a relatively short term, new energy-conversion technologies are mandatory. It is obvious that present observed trends in energy supply and consumption do not satisfy environmental sustainability. To fulfil this requirement, the participation of 10 countries has recently made it possible to establish a Generation IV International Forum (GIF). Within this framework, GIF members' have proposed the development of new generation of nuclear-power reactors to replace present technologies. The principal goals of these nuclear-power reactors, among others are: economic competitiveness, sustainability, safety, reliability and resistance to proliferation. Besides the high efficiency that should characterize such a system, it must also permit other energy applications, i.e., hydrogen production, sea water desalinisation or petroleum extraction, to be achieved. The Canadian nuclear industry is involved to develop a SCWR technology similar to actual CANDU systems that will run at a coolant outlet temperature of about 625°*C* and at pressure of 25 *MPa* [1,2]. It is important to remark that the use of pressure tubes instead of a pressure

vessel, in principle should permit the use of advanced steam-reheat thermodynamic cycles. It is obvious that at such conditions the overall efficiency of this kind of Nuclear Power Plant (NPP) will largely compete with actual supercritical water-power boilers.

In addition, from a heat-transfer viewpoint, the use of a supercritical fluid allows the limitation imposed by Critical Heat Flux (CHF) conditions, which characterize actual technologies, to be avoided. Furthermore, it will be also possible to use direct thermodynamic cycles where the supercritical fluid expands right away in a turbine without the necessity of using intermediate steam generators and/or separators. Encouraged by these facts, the conventional power industry has implemented supercritical water boiler in the 50's and 60's [3]. These fossil-fuelled units reached thermal efficiencies higher than 40% with supercritical water at about 25 *MPa* and 600°*C*. However, there is still a great amount of work that must be carried out to establish the most reliable and optimal thermodynamic-cycle topology that should be appropriate to future pressure-channel SCWRs.

Similarly to the conventional power industry, reheating the working fluid in a nuclear reactor core constitutes an excellent way for increasing the thermodynamic performance of nuclear power plants. Even though this is a common process in fossil fuelled power plants, from a neutronic view point it represents major scientific and technological challenges. However, this technology which implies complex design of reactor cores is not new; it has its germs in Russia in the earliest 1950s [4]. Based on this previous work, the pressure-channel-type of nuclear reactor seems to be the most suitable design as compared with pressurized-vessel systems. The use of independent flow channels makes it possible to implement multiple coolant passages across the reactor core. Thus, they can be subdivided at least in two different groups of fuel channels; one for heating the water up to supercritical conditions and a second group where a coolant reheat can take place. In 1964 a first 100-MW_e nuclear reactor that used steam-reheat was constructed in Russia; a second unit of 200-MW_e followed up in 1967 [4]. The gross thermal efficiency of these two nuclear power plants was about 37-38%.

Russian experiences have demonstrated the possibility of using nuclear-core reheat cycles for industrial application. It is apparent, however, that too much work is still necessary to adapt some of these concepts for designing and implementing reheat-SuperCritical Water-cooled Reactor Nuclear Power Plants (SCWR NPPs). To this end, this paper presents two possible cycle configurations for 1200- *MW* SCWR NPPs. Both cases are developed based on a Russian 660-*MW* fossil-fuelled power plant project that is intended to run under supercritical water conditions [5]. It will be constructed near the Tom'-Usinsk site, which already have nine coal-power units with a total capacity of 1272-*MW*. The commissioning of this power plant is expected to take place somewhere along 2011-2012.

2 POWER PLANT SIMULATION AND OPTIMIZATION METHOD

Improving both thermal efficiency and mechanical power, which from the optimization view point are two objective functions, constitutes a multi-objective optimization problem [6]. It is obvious that these two objectives are in competition and cannot be satisfied by a unique choice of decision variables. Thus, trade-offs between thermal efficiency and mechanical power must be determined. To this aim, in this paper an efficient and robust evolutionary algorithm based on the use of genetic algorithms [7,8] is developed and used. This tool is able to determine non dominated "optimal" solutions that conforms a Pareto's front [9]. This optimization technique is coupled to appropriate power plant thermodynamic simulation models written in Matlab (version R2009b). The plant simulator uses the X-Steam library [10] based on IAPWS-97 correlations and it communicates with the optimizer via a "Dynamic Data Ex-

change"[1] protocol (Figure 1). The optimizer generates an initial random population of solutions that are then used by a power plant simulation to evaluate thermodynamic states that are invoked to calculate objective functions and constraints required to run, once again, the optimizer. Based on the fitness of the solutions, the best ones are selected to pass crossover and mutation operators [7] to reproduce a new population of solutions that should be more efficient than the initial one. This new set seeds the simulator and the process continues until a convenient stop criterion is reached [6,8].

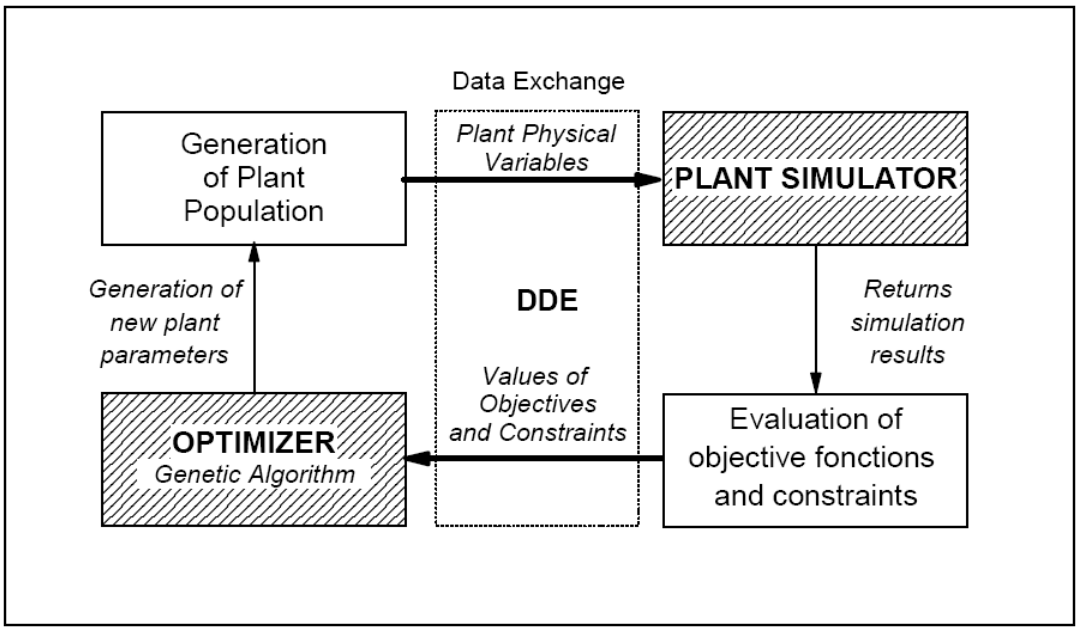

Figure 1. Plant optimization-simulation procedure.

2.1 Plant simulator and thermodynamic modelling

In this paper a reengineering process to adapt a projected supercritical water fossil fuelled plant given in [5] to a 1200-*MW* SCWR NPP is proposed. The schematic of the original system is shown in Figure 3. It consists of three turbines running in tandem within a supercritical water reheat-thermodynamic cycle. Supercritical water conditions are: $600^{o}C$ and 30 *MPa* and the expected plant thermal efficiency is close to 51%. It is interesting to note that the high pressure circulation pump (CP in the figure) is driven by a small steam turbine. Furthermore, the system is able to regenerate waste heat from gas streams through two Gas Cooling heat exchangers (GCHP and GCLP in the figure).

Before adapting this cycle to a SCWR NPP, the power plant is simulated and optimised using the method presented in Section 2. To this purpose, the X-Steam library is first validated by comparing predicted thermodynamic values with those given in the steam-table of Schmidt [11]. Relative differences, defined with respect to the values of this table are partially compared in Figure 2. In general, it is observed that the X-Steam library implemented in Matlab systematically underestimate (slightly) both enthalpies and entropies, however, maximum differences of about 1% only occur within a limited region characterized by temperatures ranging from 375 to $385^{o}C$. In addition, the proposed methodology is also validated by comparing the results of overall plant simulations with available data [5]. Even though the supercritical fossil fuelled plant shown in Figure 3 is considered as a reference case, to fulfill the objective of this work (i.e., a SCWR NPP of 1200-*MW*) it must be slightly modified.

[1] Trade mark of Microsoft Co.

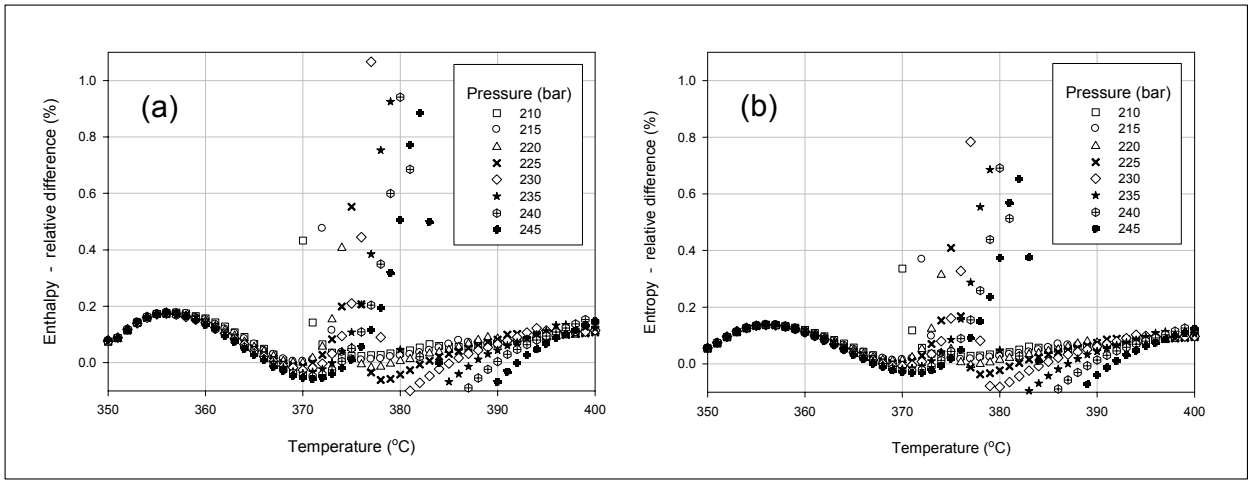

Figure 2. Comparison of water-steam properties predicted by X-Steam [10] with values given in Schmidt [11] (a) Relative enthalpy difference;
(b) Relative entropy difference.

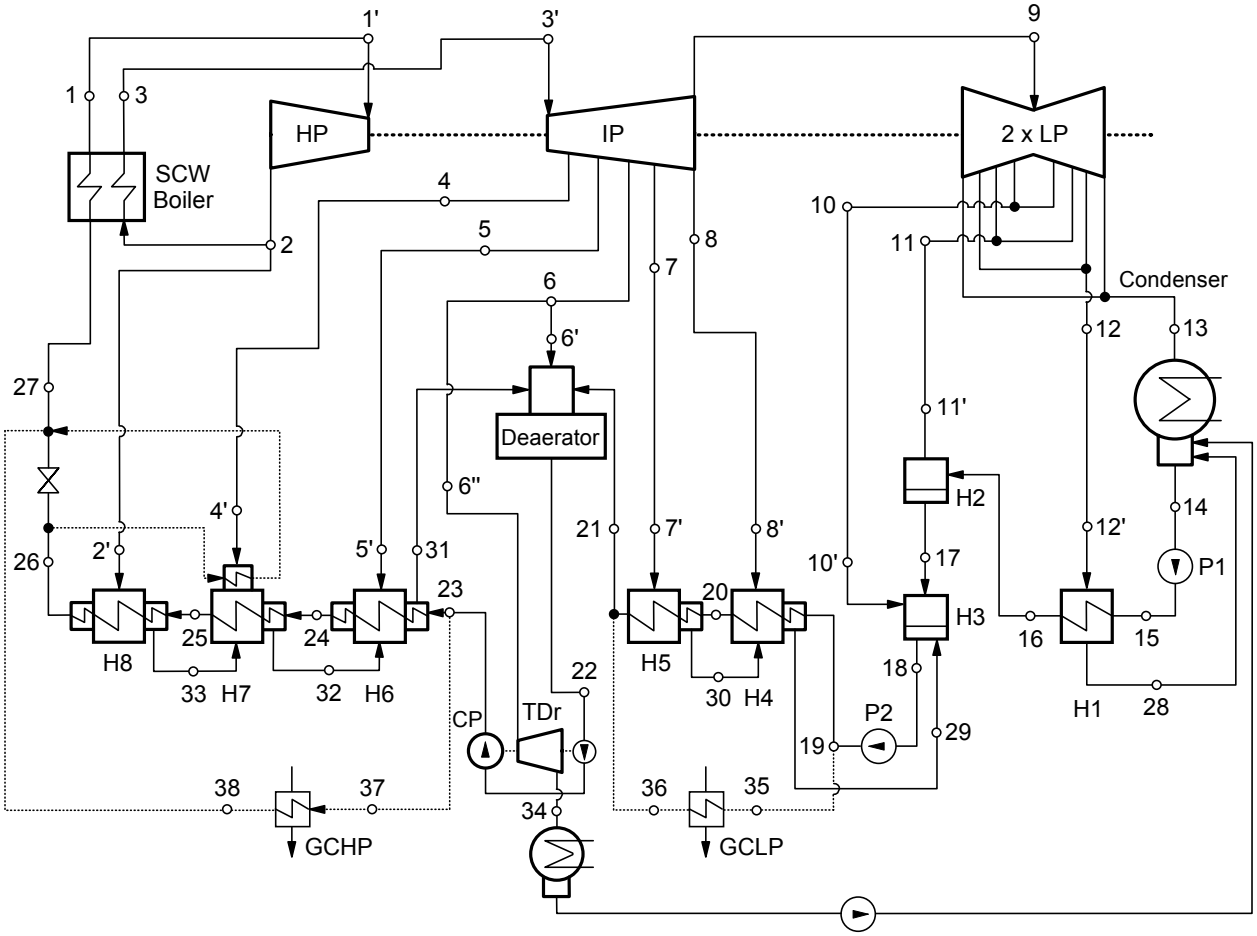

Figure 3. 669-MW_e Tom'-Usinsk Russian supercritical water fossil fuelled plant [5].

Furthermore, to satisfy the stipulated power, two different nuclear plant configurations are proposed where the SCW boiler in Figure 3 is replaced by two-pass coolant SCW nuclear reactor cores with outlet fluid conditions of 625°C and 25 *MPa* [4]. The first configuration uses two identical units of 600-*MW* each, while the second one corresponds to a plant similar to Figure 3, where the mass flow rate distributions along the cycle have been consequently increased. The power plant simulator includes specific models of different thermal equipments describe in next paragraphs.

Each turbine shown in Figure 3 is divided into multistage groups according to steam extraction points as presented in Figure 4. In the plant model, each group is characterised by an isentropic efficiency expressed as:

$$\eta_s = \frac{h_i - h_{i+1}}{h_i - h_{s,i+1}} \tag{1}$$

where $h_{s,i+1}$ represents the isentropic specific enthalpy calculated using values given in [1]. Thus, the mechanical power produced by the turbine is calculated as:

$$\left|\dot{W}_T\right| = \dot{m}\left[\left(h_o - h_1\right) + \sum_{i=1}^{n-1}\left(1 - \sum_{k=1}^{i} y_k\right)\left(h_i - h_{i+1}\right)\right] \tag{2}$$

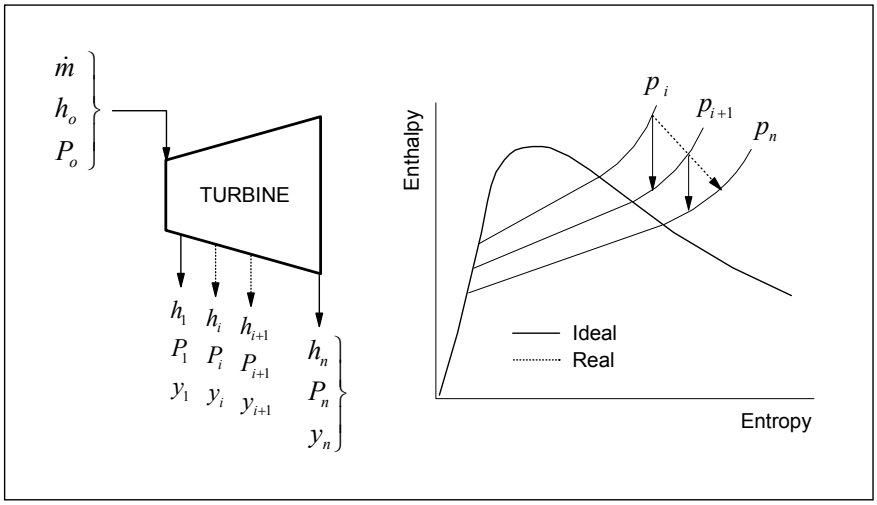

Figure 4. Simple modelling of multistage turbine groups.

Feedwater heaters permit the plant thermal efficiency to be increased by regenerating the latent heat of extracted steam fractions. The model used for closed feedwater heaters is based on temperature differences between the extracted steam and the feedwater [12]. The Terminal Temperature Differences (TTD) and Drain-Cooler Approach (DCA) used in the simulations are calculated from actual plant operation conditions given in [1]. The scheme of the three-zone feedwater heater is shown in Figure 5. Instead, for open feedwater heaters, it is assumed that at the outlet the water reaches saturated liquid state. For the deaerator (Fig. 3), saturation conditions which allow non-condensable gases to be extracted are assumed. Fur-

ther, all simulations are performed for a constant condenser pressure of 3 *kPa* and by assuming that the condensate exits this unit as saturated liquid.

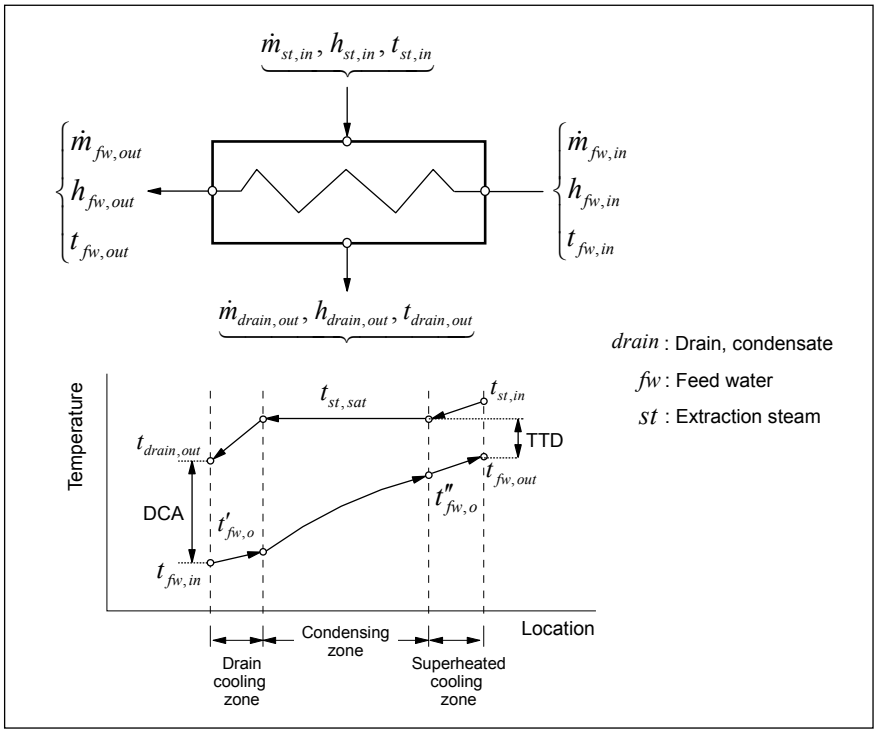

Figure 5. Flow diagram and temperature profiles of a three-zone feedwater heater.

The model of condensate pumps (P1 and P2 on Fig. 3) is performed by using the specific volume of the fluid determined at the inlet side; these pumps are considered to be ideally isentropic. In turn, the model of the high capacity circulation pump (CP on Fig. 3) takes into account the isentropic efficiency, which was determined as 78.8% by the following expression:

$$\eta_s = \frac{h_i - h_{s,i+1}}{h_i - h_{i+1}} \tag{3}$$

The reference system given in [5] provides information about pressure losses along the steam extraction lines. Notice that the thermodynamic states which are affected by these losses are indicated with primes in Figure 3. To take them into account, the simulation model must use appropriate relationships as function of the mass flow rate. Thus, in this work the following proportionality is considered as suitable:

$$\Delta P \, \alpha \, \dot{m}^2 \tag{4}$$

then a pressure loss coefficient for each line is estimated as follow:

$$coef_{\Delta P} = \frac{\Delta P_{reference}}{\dot{m}^2_{reference}} \tag{5}$$

It is assumed that this coefficient characterizes each pipe (i.e., diameter, wall roughness fraction, etc.); therefore, the pressure drop caused by different flow rates than those given in the reference case are estimated as:

$$\Delta P_{new} = \dot{m}^2_{new} \times coef_{\Delta P} \tag{6}$$

For the second 1200-*MW* SCWR NPP configuration, a single cycle based on the scheme shown in Figure 3, is proposed with a total mass flow rate increased by a factor $k > 1$. However, to maintain pressure drops as close as possible to the reference values [5], the $coef_{\Delta P}$ is divided by k^2.

3 SIMULATION AND VALIDATION PROCEDURES

For validation purposes, the original power plant given in [5] is first simulated and optimized by using the aforementioned methodology. Table 1 summarizes the reference thermodynamic states as function of the corresponding numbers shown in Figure 3. The simulation is performed by assuming a deaerator absolute pressure of 1.01 *MPa* and an absolute condenser pressure of 0.003 *MPa*. Further, outlet fluids from the deaerator, the condenser and open feedwater heaters are assumed to be under saturation liquid conditions. All other states are determined by mass and energy balances, or by using the relation between isentropic efficiencies and enthalpies (i.e., in turbines and circulation pumps).

The models used for the condenser and feedwater heaters, however, require conserving simultaneously both energy and mass; therefore, an iterative calculation is implemented [12]. Since the overall model also includes the pressure drop along lines and they may affect local thermodynamic states, an external iteration of the whole system of equation is also used. In all the cases a single convergence criterion of 10^{-6} is applied. The net mechanical power $\dot{W}$ is calculated by subtracting the power consumed by the pumps from that generated by the turbines. The plant thermal efficiency is obtained from the total thermal power input $\dot{Q}_{in}$, hence:

$$\dot{Q}_{in} = \dot{m}\left(h_1 - h_{28}\right) + \dot{m}_3\left(h_3 - h_2\right), \quad \eta = \frac{\dot{W}}{\dot{Q}_{in}} \tag{7}$$

It must be pointed out that the gas cooler units (GCHP and GCLP) shown in Figure 3 as well as the reheat line on the top of heat exchanger H7 are not included in the proposed SCW NPP configurations (they are shown by dashed lines in Fig. 3).

Table 1. Reference and simulated values of the fossil fuelled power plant given in [5].

	Reference Values					Simulated Values				
State #	$\dot{m}$ (kg/s)	T (°C)	P (MPa)	h (kJ/kg)	y (%)	$\dot{m}$ (kg/s)	T (°C)	P (MPa)	h (kJ/kg)	y (%)
1	475.9	600.0	30	3447.0		475.89	600.00	30.0	3446.87	
1'	475.9	597.0	29	3447.0		475.89	597.00	29.0	3446.87	
2	475.9	375.4	7.5	3079.4		475.89	375.20	7.5	3079.48	
2'	38.8	372.9	7.2	3079.4		38.70	372.83	7.2	3079.48	
3	437.1	620.0	7.3	3695.7		437.20	620.00	7.3	3695.84	
3'	437.1	619.7	7.2	3695.7		437.20	619.67	7.2	3695.84	
4	20.8	541.1	4.6	3534.5		20.80	541.30	4.6	3534.51	
4'	20.8	540.3	4.4	3534.5		20.80	540.47	4.4	3534.51	
5	29.1	457.9	2.7	3366.2		29.10	457.80	2.7	3366.21	
5'	29.1	457.2	2.6	3366.2		29.10	457.25	2.6	3366.21	
6	51.1	330.2	1.1	3113.7		51.10	330.10	1.1	3113.71	
6'	19.6	329.3	1	3113.7		19.60	329.07	1	3113.71	
6"	31.5	328.8	0.97	3113.7		31.50	328.76	0.97	3113.71	
7	9.1	235.3	0.5	2930.3		9.10	235.20	0.5	2930.32	
7'	9.1	234.7	0.471	2930.3		9.10	234.68	0.471	2930.32	
8	18.2	191.9	0.333	2847.4		18.30	191.80	0.333	2847.42	
8'	18.2	191.3	0.314	2847.4		18.30	191.36	0.314	2847.42	
9	308.8	191.6	0.32	2847.4		308.70	191.50	0.32	2847.42	
10	13.4	NA	0.104	2655.7	0.93	13.50	100.70	0.104	2655.71	0.93
10'	13.4	NA	0.097	2655.7	0.79	13.50	98.74	0.097	2655.71	0.79
11	13.6	NA	0.043	2530.9	4.68	13.50	77.60	0.043	2530.90	4.67
11'	13.6	NA	0.04	2530.9	4.56	13.50	75.88	0.04	2530.90	4.54
12	17.3	NA	0.018	2422.9	7.67	17.30	57.80	0.018	2422.90	7.71
12'	17.3	NA	0.0167	2422.9	7.55	17.30	56.21	0.0167	2422.90	7.58
13	264.4	NA	0.003	2267.6	11.35	264.40	24.10	0.003	2267.60	11.35
14	313.2	24.1	0.003	100.9		313.30	24.10	0.003	100.99	
15	313.2	24.1	0.49	101.7		313.30	24.10	0.49	101.48	
16	**313.2**	**53.0**	**0.39**	**222.3**		**313.30**	**52.90**	**0.39**	**221.94**	
17	326.9	76.1	0.04	318.6		326.80	75.90	0.04	317.66	
18	367.6	98.8	0.097	414.1		367.80	98.70	0.097	413.77	
19	367.6	99.0	1.37	415.7		367.80	98.80	1.37	415.09	
20	321.8	131.9	1.27	555.2		321.90	131.90	1.27	555.01	
21	367.6	147.4	1.18	621.3		367.80	147.40	1.18	621.36	
22	475.9	180.3	1.01	764.5		475.90	180.34	1.01	764.59	
23	475.9	187.1	34.3	811.8		475.90	187.20	34.3	811.90	
24	440.8	231.6	34	1006.1		440.80	231.60	34.0	1006.32	
25	440.8	NA	33.7	1107.4		440.80	254.10	33.7	1107.68	
26	440.8	289.8	33.3	1277		440.80	289.80	33.3	1276.61	
27	**475.9**	**295.0**	**33.2**	**1302.5**		**475.90**	**294.90**	**33.2**	**1302.15**	
28	17.3	56.0	0.017	234.5		17.30	56.22	0.017	235.31	
29	27.4	109.0	0.31	457.2		27.40	108.80	0.31	456.51	
30	9.1	141.9	0.47	597.5		9.10	141.90	0.47	597.26	
31	88.7	197.1	2.6	839.9		88.60	197.20	2.6	840.25	
2	59.6	241.6	4.4	1045.4		59.50	241.60	4.4	1045.50	
33	38.8	264.0	7.2	1154.3		38.70	264.10	7.2	1154.64	
34	31.5	NA	0.006	2405.3		31.50	36.20	0.006	2405.27	
35	**45.8**	**99.0**	**1.37**	**415.7**		**45.80**	**98.82**	**1.37**	**415.09**	
36	**45.8**	**147.4**	**1.18**	**621.3**		**45.80**	**147.41**	**1.18**	**621.45**	
37	**35.1**	**187.1**	**34.3**	**811.8**		**35.10**	**187.20**	**34.3**	**811.90**	
38	**35.1**	**295.0**	**33.2**	**1302.5**		**35.10**	**294.93**	**33.2**	**1302.11**	

NA Not available

The aforementioned modifications, however, have an impact on both mass and energy balances, in particular for the fraction of extracted steam due to the short of energy provided by the GCHP and GCLP systems. To overcome this drawback and for validation purposes, the gas coolers were replaced by an external heat source. Therefore, the enthalpy differences across the corresponding heat exchangers as well as the feedwater mass flow rates are kept constant. Using the reference values shown in Table 1 yields:

$$\dot{Q}_{GCLP} = \dot{m}_{35}\left(h_{36} - h_{35}\right) = 9.42\,MW\,, \quad \dot{Q}_{GCHP} = \dot{m}_{37}\left(h_{38} - h_{37}\right) = 17.21\,MW \tag{8}$$

Similar calculations performed in the reheat section shown on the top of the heat exchanger H7 (Fig. 3) resulted in 11.24 *MW*. The results of the simulation of the original power plant are shown in the first five columns on the left side of Table 1. In general, the proposed model reproduces quite well the actual operation conditions of the plant. The difference observed at state 16 is mainly due to the assumption made on the saturated liquid condition at the outlet of the heat exchanger. Indeed, the enthalpy given in the reference is higher than the value of the enthalpy at saturation for the pressure given for this thermodynamic state. Other states shown in boldface in Table 1 correspond to those used for replacing the gas cooling units (GCHP and GCLP). These states are not used for the simulation-optimization to be performed on the proposed SCWR NPPs.

The Table 1 shows that the highest difference among calculated mass flow rates is less than 1%. In turn, for temperatures and enthalpies the highest difference is lower than 0.4%. Moreover, both the thermal efficiency and the mechanical power are reproduced with much higher accuracy. These results confirm the good performance of the plant simulator; thus, it can now be used for optimization purposes.

4 RESULTS OF PLANT OPTIMIZATIONS

Once the plant modelling method is validated against available power plant data, it is used to perform the optimization of the reference case [5] as well as the proposed SCWR NPP configurations. It is apparent that a multi-objective optimization procedure must handle a large number of decision variables and constraints. In this work, pressures at different locations along the power cycle are considered as decision variables. Constraints are imposed based on temperature differences to satisfy the second law of thermodynamics. For all the cases studied, the most important values of decision variables and constraints are summarized in Table 2. The same temperature constraints used for running the reference case are also used to treat the other ones, while the qualities x_{14}, x_{17}, x_{18} and x_{22} are forced to zero. Furthermore, for all cases treated, the mass flow rate at state 12 in Figure 3 is used as an additional decision variable. It is obvious that to satisfy the optimum values of the pressures, the optimizer forces the associated mass flow rates to change. This is an important point that should be considered in future reengineering work.

The Pareto's front obtained for the reference case is shown in Figure 6. It is interesting to observe that the actual operation conditions of this fossil fuelled power plant are quite close to Pareto's boundary (i.e., $\dot{W} = 668.7\,MW$ and $\eta = 50.8\%$), i.e., the difference with respect to the front is less than 1 point of percentage. These results clearly show that the project described in [5] seems to have been already optimized and well designed to obtain an almost optimal value of thermal efficiency. From Figure 6, it is obvious that the present optimization method provides a wider range of conditions under which the plant could perform better by

decreasing the net mechanical power or vice-versa (i.e., two competing objectives). The final selection of best trade-offs must follow not only economical conditions (reduce fuel expenditures with decreasing the net available power) but technical criteria that were used for designing the plant, (i.e., turbines, heat exchangers, condenser, etc.).

Table 2. Optimization decision variables and constraints.

Decision Variables: Pressure (*MPa*)		
Reference Case 668-*MW* Fossil Fuelled Supercritical Power Plant [5]	Proposed SCWRNNP's 600-*MW* and 1200-*MW*	Temperature Constraints (^oC) All Systems
$6.6 \le P_2 \le 9.0$	$5.0 \le P_2 \le 6.5$	$tsat_{H8} - t_{33} > 0$
$3.6 \le P_4 \le 6.5$	$3.5 \le P_4 \le 4.8$	$tsat_{H7} - t_{32} > 0$
$1.5 \le P_5 \le 3.5$	$1.2 \le P_5 \le 3.4$	$tsat_{H6} - t_{31} > 0$
$0.4 \le P_7 \le 0.8$	$0.4 \le P_7 \le 0.8$	$tsat_{H5} - t_{30} > 0$
$0.2 \le P_8 \le 0.4$	$0.2 \le P_8 \le 0.4$	$tsat_{H4} - t_{29} > 0$
$0.07 \le P_{10} \le 0.20$	$0.07 \le P_{10} \le 0.20$	
$0.03 \le P_{11} \le 0.06$	$0.03 \le P_{11} \le 0.06$	
$0.015 \le P_{12} \le 0.02$	$0.015 \le P_{12} \le 0.020$	

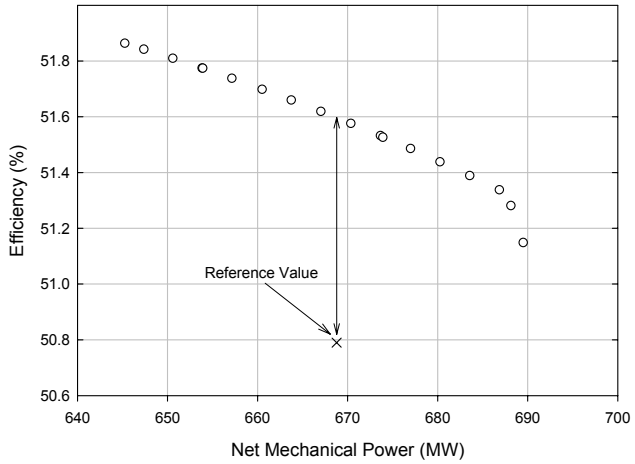

Figure 6. Pareto's front obtained for the reference case [5].

For the SCWR NPP cases, temperatures, pressures and mass flow rates are different than the reference case. In particular, pressures and temperatures are modified to satisfy the anticipated operation conditions of future SCWR's [1,2]. Thus, the pressure in the reactor core is fixed to 25 *MPa* and the outlet fluid temperature to 625°*C*. During the reheat process, however, the pressure during the second passage of the fluid in the reactor core is much lower than 6.5 *MPa*.

The Pareto's front obtained for the proposed SCWR NPP configurations as well the values obtained from the simulations before the optimization is performed, are shown in Figures 7a and 7b. For two 600-*MW* SWCR units running in parallel (Fig. 7a) a steam mass flow rate by loop of 412 *kg*/*s* is used; for the 1200-*MW* system (Fig. 7b) this value is doubled.

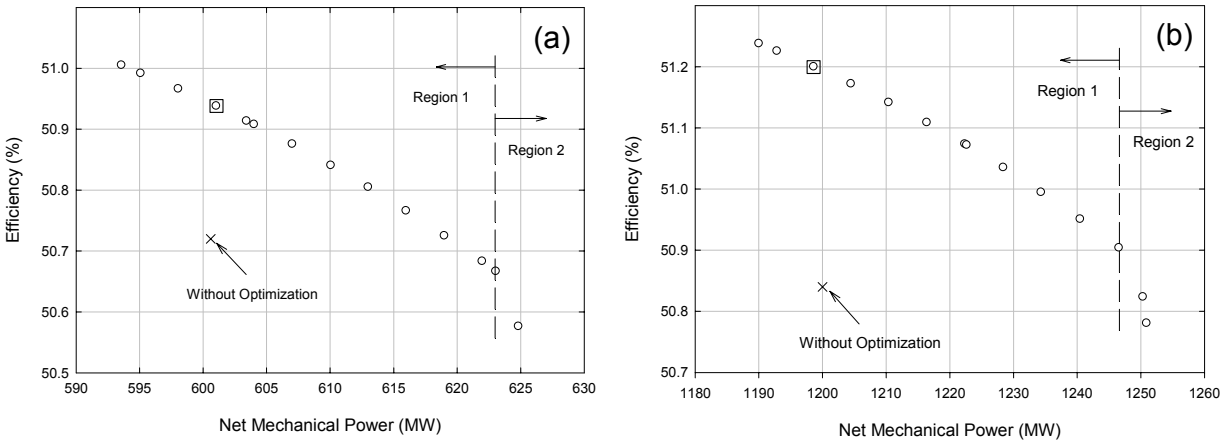

Figure 7. Pareto's front for SCWR NPP's: (a) 600-*MW* units; (b) single 1200-*MW* unit.

It is apparent that for a net mechanical power equal to the non-optimized one, the optimization permits increasing the efficiency by about 0.2 and 0.35 points of percentage respectively. Once again, it is observed that both the optimum values of efficiency and net power vary in opposite directions. The results of these cycle simulations and optimizations for a net power close to the stipulated values (points signposted on the Pareto's front in Figure 7) are given in Table 3. For both optimizations the results are very close, indeed the thermal efficiency is higher by about 0.2 points of percentage for the single 1200-*MW* unit. It may be explained by the higher temperature at the inlet of reheat process at state 2. On the other hand, the real net mechanical power produced by the 2 X 600-*MW* units is higher by about 4 *MW*. Thus the optimization reaches almost the same global behaviour for both cycles. Broadly, values of pressure at the extractions, which are the decision variables in the optimization process, are quite similar. Whereas, the mass flow rate at the extraction of state 12 which is a decision variable, is 2.6 times higher than the value for 2 X 600-*MW* units. This fact has an impact on the value of the temperature for states 16 to 21, and can probably affect the thermal efficiency of the thermodynamic cycle.

Even though, Figures 7 are plane projections of a multidimensional space (i.e., Pareto's front), according to their slopes, can be divided in two distinct regions. Close analyses of changes observed in the decision variables during the optimization shown in Figure 7a, have shown that the first region seems to be mainly controlled by the pressure at state 2 where efficiency increases with increasing the pressure. However, the net mechanical power decreases with increasing the same pressure. It is also observed that the corresponding mass flow rate of extracted steam tends to increase. This change increases feedwater reheating which in turn increases the water enthalpy at the entrance of the reactor core. This behaviour is directly correlated to the thermal efficiency of the cycle. Instead, the second region follows a more complex behaviour that seems to be controlled by pressures at state 4 and 5 and by the mass flow rate of extraction 12 (Fig. 3). Even though other variables also vary during the process, no apparent correlation between them and the Pareto's landscape was able to be established.

For the second SCWR NPP configuration, the change in mass flow rate affects the overall mass balances along the cycle. Figure 7b shows that the Pareto's front can be also divided into two regions. The behaviour of the several decision variables is quite similar to the previous case (Fig. 7a), i.e., region 1 is mainly controlled by the value of pressure at state 2 as shown in Figure 8a. Thus, efficiency increases and net mechanical power decreases with in-

creasing the pressure. Increasing the reheat pressure allows a higher temperature average during heat-addition process which is a common way for increasing the thermal efficiency in a Rankine cycle. For this case, it is also observed that within a very limited range, the efficiency is essentially affected by the extractions at states 2 and 12 (see Fig. 3), while the effects of variations on other mass flow rates are negligible. Figure 8b shows the variation of the mass flow rate at state 2 which as the previous case reheats the feedwater through the last heat exchanger. In the same way than increasing the pressure, it allows a higher temperature average for heat-addition process and thus has the effect to increase the thermal efficiency of the cycle. The second region seems to be controlled by the pressure at the first steam extraction in the IP turbine while all other decision variables remain almost constant in this region.

Table 3. Simulation-optimization results for reference case and proposed SCWR NPP's.

	Initial Values for Fossil-fuelled Power Plant [5]			Optimised Values for 2 x 600-*MW* SCWR NPP			Optimised Values for 1200-*MW* SCWR NPP		
State #	T (°C)	P (MPa)	$\dot{m}$ (kg/s)	T (°C)	P (MPa)	$\dot{m}$ (kg/s)	T (°C)	P (MPa)	$\dot{m}$ (kg/s)
1	600.0	30.0	475.9	625.0	25.00	412.0	625.0	25.0	821.3
2	375.4	7.5	475.9	394.9	6.11	34.0	399.6	6.3	69.2
3	620.0	7.3	437.1	625.0	5.96	378.0	625.0	6.05	752.1
4	541.1	4.6	20.8	534.4	3.50	11.1	532.7	3.50	21.8
5	457.9	2.7	29.1	466.8	2.27	23.2	466.3	2.29	45.7
6	330.2	1.1	51.1	361.3	1.10	51.1	359.8	1.10	51.1
7	235.3	0.5	9.1	236.9	0.40	10.1	235.7	0.40	15.4
8	191.9	0.333	18.2	182.6	0.24	17.5	195.6	0.28	28.0
9	191.6	0.32	308.8	182.2	0.23	264.9	195.3	0.23	590.1
10	100.7	0.104	13.4	89.9	0.07	11.7	110.4	0.10	14.8
11	77.6	0.043	13.6	65.8	0.026	10.0	85.8	0.0597	10.0
12	57.8	0.018	17.9	54.0	0.015	10.6	54.0	0.015	55.5
13	24.1	0.003	264.4	24.1	0.003	232.6	24.1	0.003	509.7
14	24.1	0.003	313.2	24.1	0.003	272.0	24.1	0.003	572.6
16	53.0	0.39	313.2	44.7	0.39	272.0	76.1	0.39	572.6
17	76.1	0.04	326.9	64.4	0.02	282.0	85.6	0.06	582.6
18	98.8	0.097	367.6	87.8	0.06	321.3	100.1	0.10	640.8
19	99.0	1.37	475.9	87.9	1.37	321.3	100.2	1.37	640.8
23	187.1	34.3	475.9	186.0	28.22	412.0	186.2	29.30	821.3
24	231.6	34.0	440.8	223.0	28.00	412.0	223.0	29.00	821.3
25	254.0	33.7	440.8	239.6	27.77	412.0	239.3	28.70	821.3
26	289.8	33.3	440.8	276.2	27.47	412.0	277.0	28.30	821.3
27	295.0	33.2	475.9	276.2	27.47	412.0	277.0	28.30	821.3
η **(%)**		50.79			50.94			51.20	
$\dot{W}$ (*MW*e)		668.78			601.06			1198.66	

In general it is observed that the improvement in the mechanical power can be substantial, while conditions imposed by the deaerator limit considerably the possibility to enhance plant's efficiency. These conditions, however, are necessary to guarantee acceptable removal of non-condensable gases.

From an engineering view point, the first SCWR NPP configuration will necessitate doubling mechanical and nuclear components which will increase both investment and operational cost. In turn, the fact that the second configuration requires much higher mass flow rates, will involve different dimensioning of major thermal components, i.e., turbines, heat exchangers, condenser, etc. A trade-off between these two possibilities will still necessitate a multi-objective optimization that should include appropriate economic models.

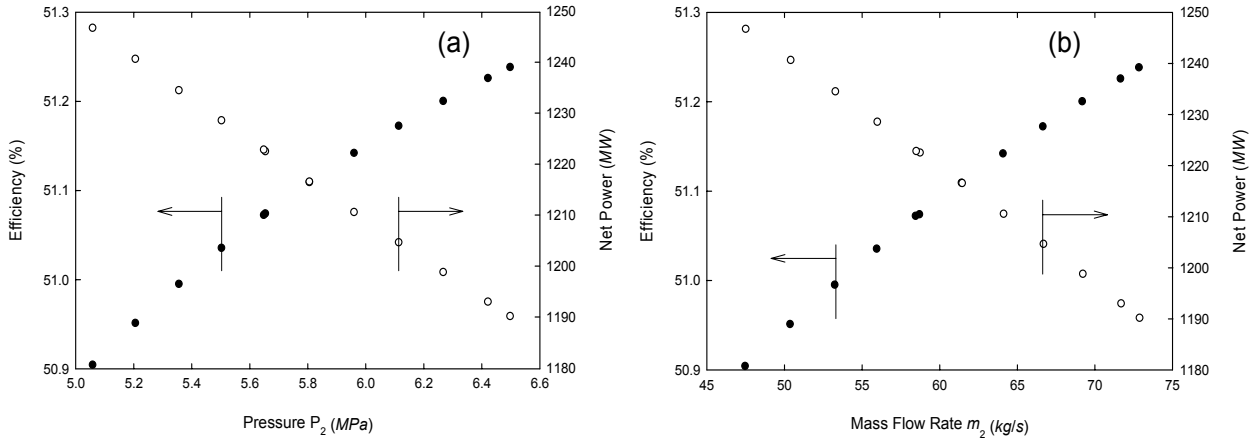

Figure 8. Variations of efficiency and net power: (a) as a function of pressure P_2; (b) as a function of mass flow rate $\dot{m}_2$.

5 CONCLUSION

A plant modelling approach coupled to an evolutionary optimization technique is presented. The model is validated by comparing its prediction with data taken from a projected Russian fossil fuelled supercritical water plant. The same model and plant layout are then slightly modified and used to produce suitable topologies for future SCWR NPP based on core coolant-reheat cycles. The first option, which consists of two 600-*MW* units running in parallel, needs a total water mass flow rate of 412 *kg*/*s* per loop. The optimization of such a system shows a Pareto's landscape that offer a quite large spectrum of possible operation conditions. The optimisation of the second SCWR NPP system consisting of a single 1200-*MW* unit produces a Pareto's front having similar features with a mechanical power ranging from 1190 to 1250-*MW*. In both cases it is observed that the front can be subdivided in two distinct regions where the optima seem to be controlled by only few decision variables. This observation may help process engineers in achieving more appropriate power plant designs. Even though efficiency and mechanical power are competing objective functions, the Pareto's fronts indicate that it is still possible to improve simultaneously both of them.

ACKNOWLEDGMENTS

This work is funded by the Natural Sciences and Engineering Research Council of Canada discovery grant RGPIN 41929 and the Hydro-Québec Chair in Nuclear Engineering.

REFERENCES

[1] Duffey R.B., Pioro I.L., Zhou T., Zirn U., Kuran S., Khartabil H. and M. Naidin, "Supercritical Water-Cooled Nuclear Reactors (SCWRs): Current And Future Concepts - Steam Cycle Options," *16th Int. Conf. Nucl. Eng.*, Florida, USA, 2008.

[2] Pioro, I.L. and R.B. Duffey, "Heat Transfer and Hydraulic Resistance at Supercritical Pressures in Power Engineering Applications," ASME Press, New York, 2007.

[3] Leyzerovich S., "Steam Turbines for Modern Fossil-Fuel Power Plants," Fairmont Press, Inc. Lilburn, 2008.

[4] Saltanov E., Monichan R., Tchernyavskaya E. and I. Pioro, "Nuclear Steam-reheat Options: Russian Experience," *2nd Canada-China Workshop SWCR"*, Canada, 2010.

[5] Kruglikov P.A., Smolkin Yu.V. and K.V. Sokolov, "Development of Engineering Solutions for Thermal Scheme of Power Unit of Thermal Power Plant with Supercritical Parameters of Steam," (In Russian) *Workshop Supercritical Water and Steam in Nucl. Power Eng.: Problems and Solutions*, Moscow, Russia, 2009.

[6] Dipama J., Teyssedou A., Aubé F. and L. Lizon-A-Lizon, "A Grid Based Multi-Objective Evolutionary Algorithm for the Optimization of Energy Systems," *App. Thermal Eng,* Vol. 30, pp. 807-816, 2010.

[7] Goldberg D. E., "Genetic algorithms in search, optimization, and machine learning, Reading," Addison-Wesley, 412 p., 1989.

[8] Dipama, J., « Optimisation multi-objectif des systèmes énergétiques » Thèse de Doctorat, École Polytechnique de Montréal, (Avril 2010).

[9] Pareto V., « Cours d'économie politique », F. Rouge editor, Lausanne (1896).

[10] M. Holmgren, "X Steam for Matlab," Edition, 2006.

[11] Schmidt E., "Properties of Water and Steam in SI-Units," Springer-Verlag, Berlin, Third Edition, (1982).

[12] Teyssedou A, Dipama J., Hounkonnou W. and F. Aubé, "Modeling and Optimization of a Nuclear Power Plant Secondary Loop," Nucl. Eng. Design, 240, pp. 1403-1416, 2010.